International Journal of Scientific Engineering and Technology Research

ISSN 2319-8885
Vol.07,Issue.10,
October-2018,
Pages:1779-1787

www.ijsetr.com

Bridgeless Multi Level Inverter for Single Phase and Three Phase Applications

V. BHAGAVATHI[1], L. KISHORE[2]

[1]PG Scholar, Dept of EEE, Sree Kavitha Engineering College, Karepalli, Telangana, India.
[2]HOD, Dept of EEE, Sree Kavitha Engineering College, Karepalli, Telangana, India.

Abstract: This paper presents a new unidirectional cascaded bridgeless multilevel rectifier (CBR) well suited for serving as the rectifier stage of a transformerless cascaded multilevel converter. Compared to a traditional cascaded H-bridge rectifier, the proposed CBR utilizes fewer fully controlled switching devices by replacing the fully controlled H-bridge modules with bridgeless PFC modules, thus simplifying the control circuits, increasing the system reliability, and cutting down the implementation expenses. However, when a single-phase CBR is operating under a unity power factor, the input current will be severely distorted because of the unidirectional power flow property of the bridgeless PFC modules. Therefore, aiming at achieving a satisfactory current quality and power factor simultaneously, an improved control strategy and a revised topology for the single-phase CBR are provided as two effective solutions. Specifically, for the single-phase CBR under the improved control, the limitation of the maximum value of the boost inductance considering an acceptable power factor is derived. Besides, the method of determining the configuration of the modified single-phase CBR is given based on the steady-state analysis. In addition, for the three-phase CBR, the reason that the traditional control strategy is capable of realizing unity power factor rectification while mitigating input current zero-crossing distortion is analyzed. Finally, simulations in the MATLAB/Simulink results are provided to verify the proposed theories.

Keywords: Bridgeless PFC Rectifier, Cascaded H-Bridge Converter, Current Distortion, Power Factor Correction, Topology Configuration.

I. INTRODUCTION

With the advancement of power semiconductor devices and other power electronics-related technologies, the emerging concept of the transformerless cascaded multilevel converter (TCMC) has rapidly developed and caught increasing attention from both the academia and industry in the past decades [1]–[9]. As shown in Fig. 1, by employing a cascaded H-bridge rectifier (CHR) as the front stage, the TCMC is able to realize direct connection to the medium/high voltage power grid without involving a bulky and expensive line-frequency transformer, thus increasing the efficiency and power density of the system. Besides, the utilization of CHR also endows the TCMC with many additional advantageous features such as improved power quality and flexible regulation of output voltage, which justify the potential of the TCMC as a renewable energy interface or a solidstate transformer [10], [11]. Related design guidance and control strategies of the TCMC have been provided in the literature. Despite all the aforementioned merits, the CHR still possesses some undesirable properties when it is used as the rectifier stage of a TCMC. The major drawbacks include high switching losses, complicated hardware system, and high implementation expenses as all the switching devices adopted in the CHR are fully controlled ones (IGBT or power MOSFET) with antiparallel diodes.

In addition, considering a TCMC intended for a higher voltage-rated application, more H-bridge modules need to be cascaded to compose the CHR, which further increases the number of fully controlled switches and inevitably leads to more complicated control, gate driving, and protection circuits.

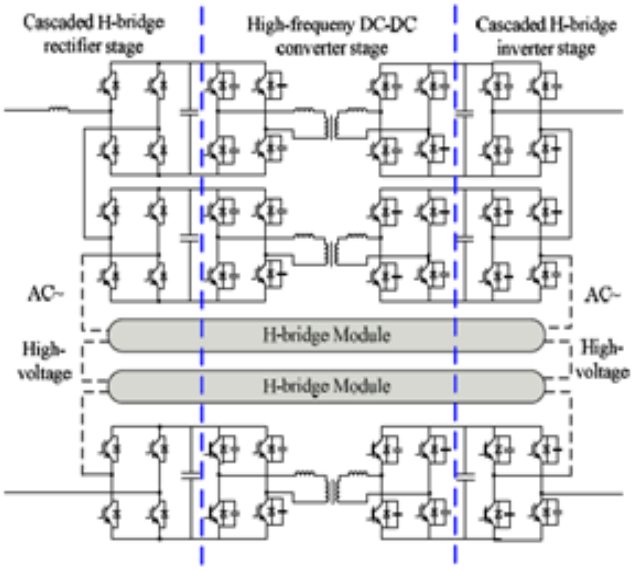

Fig.1. Topology of cascaded H-bridge converter.

This eventually reduces the system reliability and increases the implementation costs [12]–[14]. However, in nearly 70% of practical applications, including speed regulation for pumps, wind power integration, and plug-in electrical vehicle applications, only a unidirectional power flow is required. As can be seen from Fig. 2, several power modules are cascaded for direct connection to the medium voltage grid. Each of these power modules is composed of a traditional boost PFC circuit. In this way, the number of fully controlled switches is greatly reduced. However, the boost inductor of each power module is located at the dc side. Under certain conditions, the energy stored in the boost inductor can generate a circulating current that circulates through the fully controlled switch and the diodes.

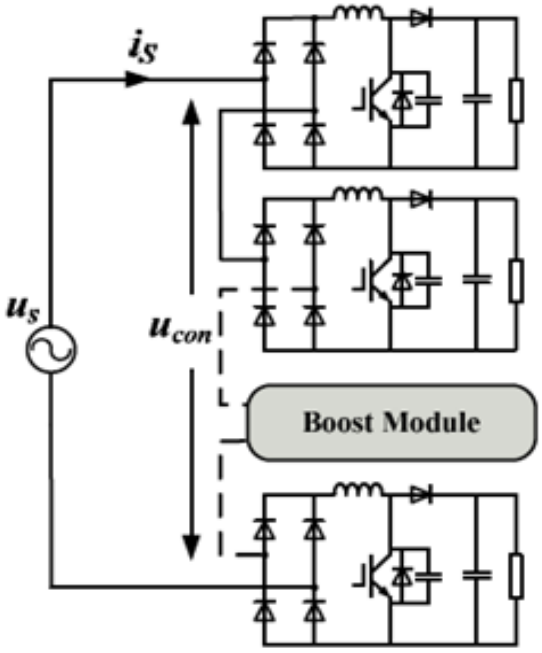

Fig.2. Topology of single-phase cascaded diode H-bridge rectifier.

Consequently, the large circulating current may damage the devices or even break down the whole system. Additionally, the power module shorted by the circulating current is actually bypassed from the power grid, thus the grid voltage has to be shared among the other cascaded modules. As a result, the voltage stresses of the switches in those modules increase greatly. Another problem is that the current is always carried through three semiconductor devices within each module, causing relatively high conduction losses. a diode H-bridge cascaded boost rectifier, the power grid is directly connected with a high voltage-rated diode H-bridge rectifier, which is in series-connection with several cascaded boost dc/dc modules. This topology also employs much fewer fully controlled switches and can effectively prevent the circulating current. The diode H-bridge rectifier, however, still has a limited input voltage rating, which makes it unable to be directly connected to the medium/high voltage power grid. It is worth pointing out that a three-phase multilevel rectifier uses three times as many cascaded modules as a same rated single-phase rectifier does.

Therefore, developing a new topology for the three-phase cascaded multilevel rectifier brings even more attractive benefits. However, no related research has been reported yet. This paper presents a cascaded bridgeless multilevel rectifier (CBR) aiming at using fewer fully controlled switches to reduce hardware complexity, increase system reliability,

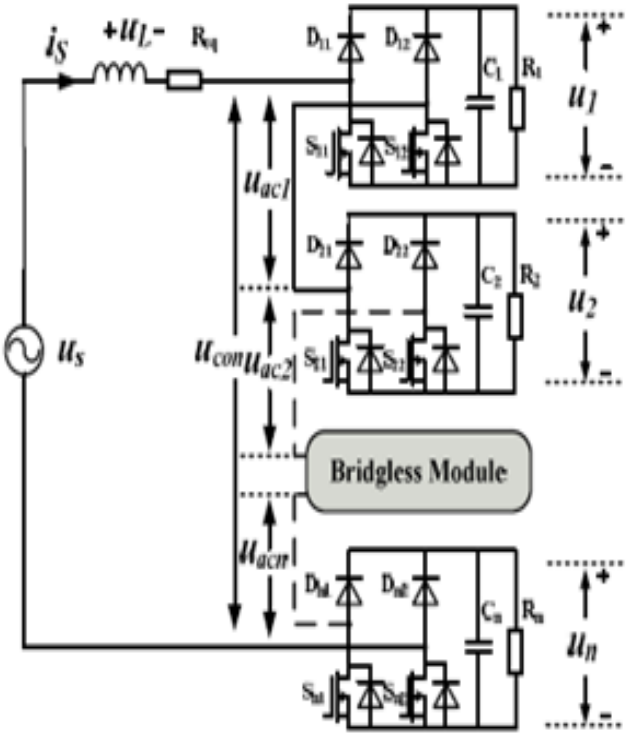

Fig. 3. Topology of single-phase CBR.

and cut down the implementation expenses. Based on analyzing the physical cause of the input current zero-crossing distortion when the single-phase CBR is operating under a unity power factor, an improved control strategy is proposed to achieve a satisfactory power factor and eliminate the input current zero-crossing distortion. Besides, a revised topology of the single-phase CBR is presented as another solution for avoiding the input current distortion under the unity power factor condition. In addition, different from the single-phase case, the three-phase CBR can achieve a unity power factor with greatly attenuated input current zero-crossing distortion by employing the traditional control method.

II. BASIC PRINCIPLES OF THE CBR

A. Topology Configuration of the CBR

Fig. 3 shows the main topology of the proposed single-phase CBR. As can be seen, n bridgeless modules are cascaded so that the rectifier can be directly connected to the medium/high voltage grid. Compared to a traditional H-bridge module, each bridgeless module reduces 50% fully controlled switches. Therefore, the control circuits, gate drivers, as well as protection units are greatly reduced, thus decreasing the system complexity and switching losses drastically. For a nonideal power converter, the ac side power loss induced by the line impedance, boost inductor ESR, and other device parasitic parameters is approximately

proportional to the square value of the input current. Hence, an equivalent series resistor Req is used to represent the ac side power loss as well as the voltage drop at the input side of the cascaded modules [10].

B. Steady-State Mathematical Model of the CBR

Define uaci and ui as the ac voltage and the output dc voltage of Module i , respectively, where i = 1, 2, . . . , n. In each bridgeless module, the two fully controlled switches are controlled by two identical gate signals. Define Si as the switching function of Module i. When Si = 1, the switching devices of Module i are turned on, while Si = 0 means the switching devices are turned off. Due to the unidirectional conduction property of the diodes, the ac voltage of Module i depends on the direction of the input current and can be derived as

$$u_{\text{aci}} = \begin{cases} (1 - S_i)u_i & i_S > 0 \\ -(1 - S_i)u_i & i_S < 0. \end{cases} \quad \textbf{(1)}$$

Applying KVL and KCL to the topology shown in Fig. 3, the steady-state mathematic model can be yielded as

$$\begin{cases} L\dfrac{di_S}{dt} = u_S - R_{\text{eq}} \cdot i_S - \sum_{i=1}^{n} S_i^* \cdot u_i \\ C\dfrac{du_i}{dt} = S_i^* \cdot i_S - \dfrac{u_i}{R_i} \end{cases} \quad \textbf{(2)}$$

where

us , is the input voltage and input current;

L the boost inductance at the ac side;

C the dc capacitance of each module;

R_{eq} the ac side equivalent series resistance;

R_i , u_i , S_i the equivalent load resistance, output voltage, and switching function of Module i. S_i = 0, 1; S*i = 1 − Si ; i = 1, 2, . . . , n.

Applying the volt-second balance and ampere-second balance principles to (1) and (2) yields

$$\begin{cases} i_s = \dfrac{u_S}{R_{eq} + \sum_{i=1}^{n} R_i(1 - d_i)^2} \\ u_i = \dfrac{u_S \cdot Ri(1 - di)}{R_{eq} + \sum_{i=1}^{n} R_i(1 - d_i)^2} \end{cases} \quad \textbf{(3)}$$

where di is the duty cycle of Module i .

Equation (3) indicates the input–output characteristics of the CBR. By modifying the duty cyclesd1, d2…dn, the output voltages of the cascaded modules and the input current of the rectifier can be adjusted. For instance, the dc voltage unbalance could appear due to the device loss mismatching and the real power differences among the cascaded modules. The unbalanced voltage will cause the capacitor and/or switch overvoltage and then trigger the system overvoltage protection. Therefore, the output dc voltages of the cascaded modules must be balanced to ensure safe and stable operation. As is implied by the mathematical relationship between ui and di, through appropriately modifying di , ui can be

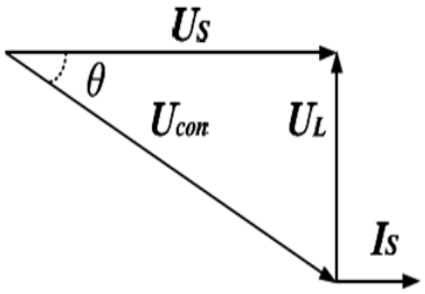

Fig.4. AC side phasor diagram of the single-phase CBR.

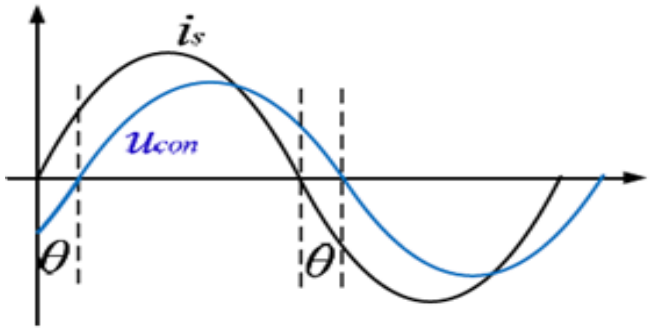

Fig.5. Theoretical relationship between iS and ucon.

controlled equal to the reference value. Actually, from the circuit point of view, di controls the charging and discharging time of the dc capacitor, thus directly influencing ui. This is a straightforward physical explanation of using di to balance the output dc voltages.

C. Power Factor Analysis of the Single-Phase CBR

Fig. 4 gives the ac side phasor diagram of the single-phase CBR. Since the ac side equivalent series resistance Req is very small, the voltage drop across it is reasonably neglected here [28]. Under the condition that the unity power factor is achieved, the input voltage US is in phase with the input current IS. The voltage across the boost inductor UL is orthogonal to IS. Ucon is the total ac voltage of the rectifier and it equals the sum of the ac voltages of all the cascaded modules. According to the triangle law of vector addition, Ucon lags IS by θ. As shown in Fig. 5, this lagging angle θ indicates that during a period of θ after the current crosses zero, the input current iS and the total ac voltage of the rectifier ucon have to be opposite in polarities. By contrast, due to the unidirectional conduction property of the iodes, the ac voltage and the input current of a single-phase CBR must always remain in the same direction. Hence, during this period of θ, the CBR can only generate a 0 V ac voltage, causing the input current iS to be

$$U_S \cos \omega t = L\frac{di_S}{dt} \quad \textbf{(4)}$$

$$i_S = \frac{U_S}{\omega L} \sin \omega t \quad \textbf{(5)}$$

where USis the magnitude of the input voltage.

Equation (5) indicates that at the zero-crossings, iS suddenly changes to be lagging behind ucon by 90, rather than

keeping in phase with ucon. Therefore, as can be seen in Fig. 6, if a single-phase CBR is forced to operate

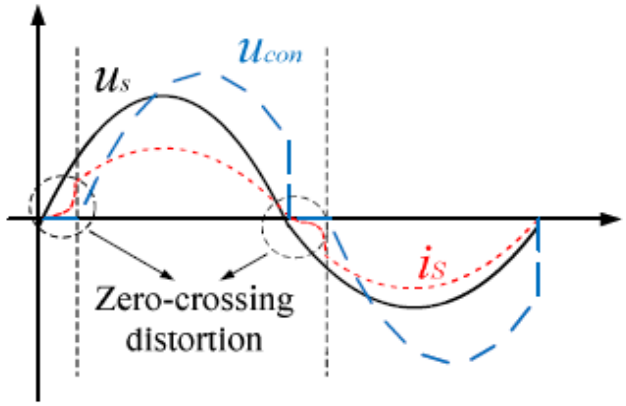

Fig.6. Input current zero-crossing distortion of the single-phase cascaded diode H-bridge rectifier.

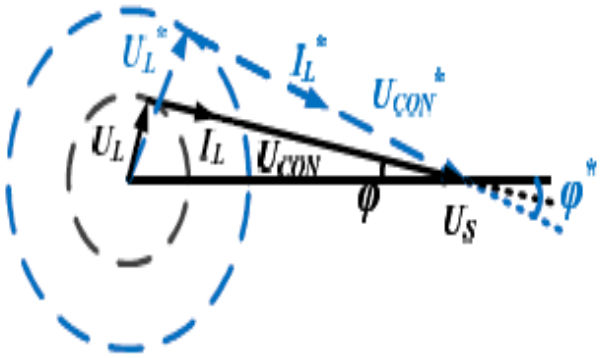

Fig.7. AC side phasor diagram of the single-phase CBR under the improved control strategy.

under the unity power factor, serious input current distortion appears at the zero-crossings. This property is defined as the input current zero-crossing distortion. Actually, the heavier the loads are, the more serious the input current zero-crossing distortion is. To address this problem, two possible solutions are provided in the following. The first solution is to employ an improved control strategy. The second option is to replace some (but not all) of the bridgeless module(s) of the CBR with H-bridge module(s).

III. IMPROVED CONTROL STRATEGY FOR THE SINGLE-PHASE CBR

A. Improved Control Strategy

The conventional CHR adopts the classical double-loop control method to make the input current in phase with the input voltage so that the unity power factor is achieved. However, this control scheme needs to be modified before it can be applied to the single-phase CBR, otherwise, the input current will be seriously distorted at the zero-crossings. The core idea of the improved control strategy is to make IS in phase with Ucon, rather than in phase with US. As can be seen from Fig. 7, applying this new control strategy results in a lagging power factor and the lagging angle ϕ increases to ϕ when the loads become heavier. By realizing the desired lagging angle, IS and Ucon can be kept in phase, thus eliminating the current distortion. The corresponding ac waveforms are shown in Fig. 8. According to the geometric relationship indicated in Fig. 7, the voltage across the boost inductor UL satisfies

$$U_L = \omega L I_S = U_S \sin\varphi \tag{6}$$

Considering the input–output power balance, (7) can be yielded as

$$\sum_{i=1}^{n} \frac{u_i^2}{R_i} = U_S I_S \cos\varphi \tag{7}$$

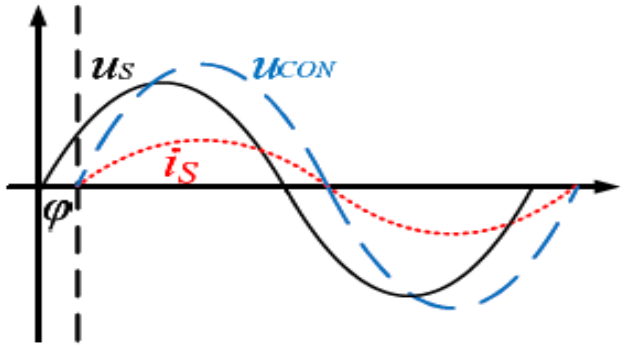

Fig.8. AC side waveforms of the single-phase CBR under the improved control strategy.

Substituting (6) into (7) and considering that the output dc voltages are well balanced in the steady state, the desired lagging angle can be yielded as

$$\varphi = \frac{1}{2}\arcsin\left(\frac{2\omega L U_d^2}{U_S^2}\cdot\sum_{i=1}^{n}\frac{1}{R_i}\right) \tag{8}$$

where Ud is the reference output dc voltage of each cascaded module.

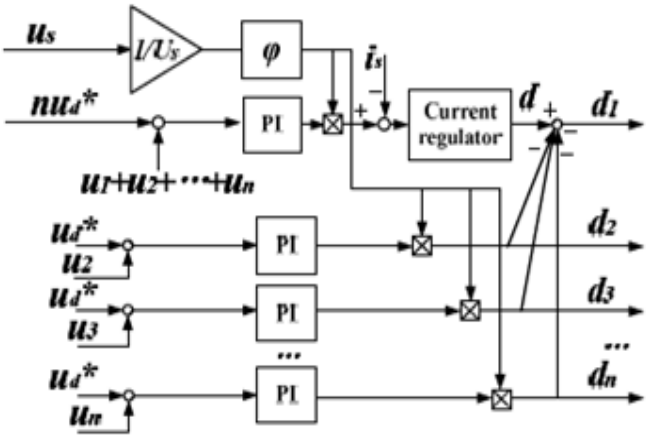

Fig.9. Block diagram of the improved control strategy for the single-phase CBR.

After obtaining the desired lagging angle, the improved control strategy can be applied to the single-phase CBR. As can be seen in Fig9, the overall voltage loop is implemented to regulate the total output voltage. The current loop generating the total duty ratio d is responsible for realizing a sinusoidal current without zero-crossing distortion by

forcing the input current to lag the input voltage by the desired angle ϕ. For Module 2 to Module n, a PI controller is applied to each module as an individual voltage regulator to make the output dc voltage equal to the reference value u∗ , thus balancing the dc voltages. Through these individual voltage regulators, the duty cycles d2 . . . dn are generated. Then the duty cycle of Module 1 is obtained by d1 = d −d2−· · ·−dn. It should be noticed that although the input current lags the input voltage by a certain angle, a satisfactory power factor for most practical applications (above 0.95) can still be ensured by limiting the maximum value of the boost inductance according to (8).

B. Maximum Boost Inductance Limitation

Usually, the minimum inductance Lmin is determined according to the allowed current ripple magnitude i_S. References [9] and [10] proposed a method that uses the minimum duty cycle of all the cascaded modules to estimate the current ripple for calculating the minimum inductance. This method is also suitable for choosing the minimum boost inductance for the CBR under the improved control. Due to the limited space, details of this minimum inductance calculating procedure are not discussed in this paper. Instead, this paper focuses on how to ensure an acceptable power factor by limiting the maximum value of the boost inductance. As stated above, the improved control strategy leads to a lagging power factor that is closely related to the boost inductance. Therefore, by properly limiting the maximum boost inductance, the power factor can be controlled above the minimum acceptable value. Define k as the minimum power factor allowed. Substituting cos ϕ = k into (8) yields the limitation of the maximum boost inductance

$$L_{\max} = \frac{U_S^2 \sin(2\cos^{-1} k)}{2\omega U_d^2 \sum_{i=1}^{n} \frac{1}{R_i}} \tag{9}$$

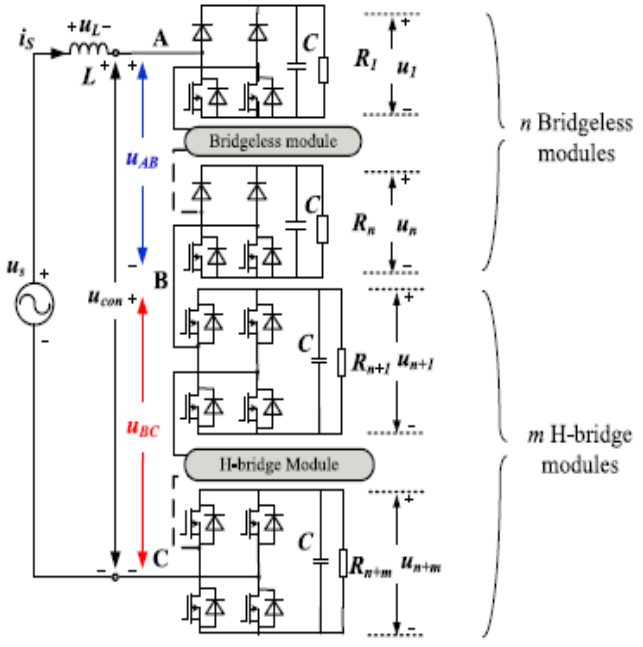

Fig.10. Topology of the revised single-phase CBR.

IV. REVISED TOPOLOGY OF THE SINGLE-PHASE CBR

A. Revised Topology

As analyzed before, the single-phase CBR is not able to achieve unity power factor rectification without a distorted input current. This is because the input current IS can only be in phase with the ac voltage of the CBR Ucon. In other words, the cascaded bridgeless modules are not able to provide the reactive power consumed by the boost inductor L when no reactive power is injected from the power grid. It should be noted that the voltage drop across the boost inductor UL is typically very small compared to Ucon and US. Therefore, one or a few more bridgeless module(s) can be replaced by conventional H-bridge module(s) to provide the needed reactive power for the boost inductor. In this way, the revised CBR can be used in the applications where the unity power factor is required. The topology of this revised single-phase CBR is shown in Fig. 10 where Module 1 to Module n are bridgeless modules and Module (n+1) to Module (n+m) are H-bridge modules, and n+m = N. uAB and uBC are the sum of the ac voltages of the bridgeless modules and the H-bridge modules, respectively. Additionally, the following equation is satisfied:

$$u_{\text{con}} = u_{\text{AB}} + u_{\text{BC}}. \tag{10}$$

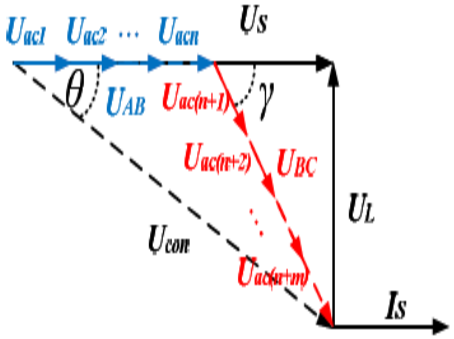

Fig.11. AC side phasor diagram of the revised single-phase CBR.

Fig. 11 shows the ac side phasor diagram (with UL exaggerated) of the revised topology. Since the unity power factor is strictly demanded, IS is in phase with US. Hence, UL is orthogonal to US. In order to avoid input current distortion, UAB has to be controlled in phase with US. Therefore, UBC must contain reactive component to provide the required reactive power for the inductor and active component to support the dc voltages. As a result, UBC lags IS by γ and Ucon lags IS by θ. Define Uaci as the ac voltage of Modulei . Then the following relationships exist:

$$\begin{cases} U_{\text{AB}} = \sum_{i=1}^{n} U_{\text{aci}} \\ U_{\text{BC}} = \sum_{i=n+1}^{m} U_{\text{aci}}. \end{cases} \tag{11}$$

UPi is defined as the active component of the ac voltage of Module i and can be expressed as

$$\begin{cases} U_{\mathrm{Pi}} = U_{\mathrm{aci}}, & i = 1, 2, \ldots, n \\ U_{\mathrm{Pi}} = U_{\mathrm{aci}} \cos\gamma, & i = n+1, \ldots, n+m. \end{cases} \quad (12)$$

Applying the geometrical relationship yields

$$\sum_{i=1}^{n+m} U_{\mathrm{Pi}} = U_S. \quad (13)$$

Considering the output dc voltages are well balanced in the steady state, the active power transferred through each module can be expressed as

$$U_{\mathrm{Pi}} I_S = \frac{U_d^2}{R_i}, \quad i = 1, 2, \ldots, n+m \quad (14)$$

According to [9], for each cascaded module, the maximum ac voltage that can be obtained through modulation is

$$U_{\mathrm{ac\,max}} = \frac{4}{\sqrt{2}\pi} U_d \quad (15)$$

It is clear that the active component of the ac voltage of ModuleiUPi must satisfy

$$U_{\mathrm{Pi}} \le U_{\mathrm{ac}} \le U_{\mathrm{ac\,max}}, \quad i = 1, 2, \ldots, n+m \quad (16)$$

B. Determination Method of the Topology Configuration

The values of n and m have to be carefully determined such that the revised CBR is able to achieve: 1) unity power factor and sinusoidal input current; 2) output dc voltage balancing; and 3) minimized value of m to reduce the fully controlled switches [29]. For the purpose of simplification,

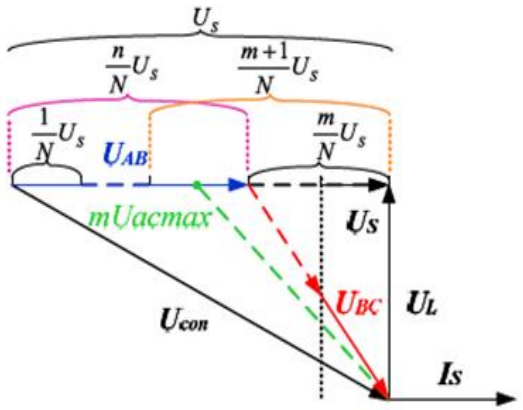

Fig. 12. AC side phasor diagram for determining the topology configuration of the revised CBR.

the configuration determination method is derived under the balanced load condition. Substituting R1 = R2 = · · · = Rn+m = R and (14) into (13) yields the relationship among the active ac voltage components of the modules

$$U_P = U_{\mathrm{Pi}} = \frac{U_S}{n+m} = \frac{U_S}{N}, \quad i = 1, 2, \ldots, n+m \quad (17)$$

Fig. 12 gives the steady-state ac side phasor diagram for determining the topology configuration. It can be seen that the total ac voltage of the m H-bridge modules UBC must be able to compose a phasor triangle with its active component and the inductor voltage UL . Hence, (18) should be met as

$$(\mathrm{m}U_P)^2 + U_L^2 = U_{\mathrm{BC}}^2 \quad (18)$$

Substituting (11) and (16) into (18) yields the constraint for the value of m

$$(\mathrm{m}U_P)^2 + U_L^2 \le (\mathrm{m}U_{\mathrm{ac\,max}})^2 \quad (19)$$

Substituting (17) into (19) gives

$$\left(U_{\mathrm{ac\,max}}^2 - \frac{U_S^2}{N^2}\right) m^2 - U_L^2 \ge 0 \quad (20)$$

Define the step-up ratio K as

$$K = \frac{\mathrm{N}U_d}{U_S} \quad (21)$$

Neglecting the power loss leads to the input–output power balance

$$U_S I_S = N \frac{U_d^2}{R} \quad (22)$$

Substituting (15), (21), and (22) into (20) and plugging in UL = ωLISyield

$$m > \frac{\omega K^2}{\sqrt{\frac{8}{\pi^2}K^2 - 1}} \frac{L}{R}. \quad (23)$$

Then the minimum integer value of m that satisfies (23) is chosen to be the number of the H-bridge modules. Therefore, n = N − m is the number of the bridgeless modules. It should be noted that Uac max > UP = US/N, therefore, the larger m is, the easier it is for (20) to be satisfied. Besides, it can be seen from (23) that m will increase if the loads become heavier. This mathematical finding agrees with the fact that when the loads are heavier, the reactive power consumed by the boost inductor L is larger, requiring more H-bridge modules to realize unity power factor operation. For the unbalanced load condition, the main idea of determining the values of n and m is the same. However, the active power transferred through Module i is inversely proportional to its equivalent load resistance Ri . As a result, (17) has to be replaced by

$$U_{\mathrm{Pi}} = n_i U_S \quad (24)$$

where ni is defined as the load unbalance ratio and is expressed as

$$n_i = \frac{\frac{1}{R_i}}{\sum_{j=1}^{N} \frac{1}{R_j}}. \quad (25)$$

Then the values of n and m can be determined following the same procedures as in the balanced load case:

$$m > \frac{\sqrt{2}\pi}{4} \sqrt{\frac{\omega^2 L^2 \left(\sum_{i=1}^{N} \frac{1}{R_i}\right)^2}{U_S^2} + \frac{N^4}{K^2}\left(\sum_{l=1}^{m} n_l\right)^2} \quad (26)$$

Similarly, the minimum integer value of m that satisfies (26) is selected to be the number of the H-bridge modules and n = N − m is the number of the bridgeless modules. Calculating n and m using (23) and (26) can be complicated. However, the voltage drop across the boost inductor is typically very small. As a consequence, for most cases, one H-bridge module should have enough capability to provide the required reactive power. Therefore, for a revised CBR composed of N modules, usually only one of them needs to be an H-bridge module.

C. Control Strategy of the Revised Single-Phase CBR

A novel control strategy based on the single-phase dq transformation is proposed for the revised CBR. Fig13 depicts the control block diagram. The error between the dc voltage reference u∗ d and the mean value of the dc voltages of all the cascaded modules is regulated by a PI controller to generate the active current referencei * d. Meanwhile, the reactive current reference i * q is set to be zero in order to achieve the unity power factor. Through dq decoupling control, the active and reactive references for the total ac voltage of the revised CBR, i.e., u* cond and u* conq, are obtained. According to (10), the ac voltage references u* AB and u*BC should meet

$$\begin{cases} u^*_{cond} = u^*_{\mathrm{ABd}} + u^*_{\mathrm{BCd}} \\ u^*_{\mathrm{conq}} = u^*_{\mathrm{ABq}} + u^*_{\mathrm{BCq}}. \end{cases} \quad (27)$$

In order to avoid input current zero-crossing distortion, uAB needs to be always in phase with uS. Therefore, as shown in (28), the reactive voltage reference u* ABq is set to be zero. As a consequence, u* BCq has to be u* conq. The output dc voltages should be balanced. Otherwise, the unbalanced voltage may result in capacitor overvoltage. Hence, the active power should be equally distributed among all the cascaded modules. Since all the modules are cascaded, the active power transferred through each module is proportional to the active

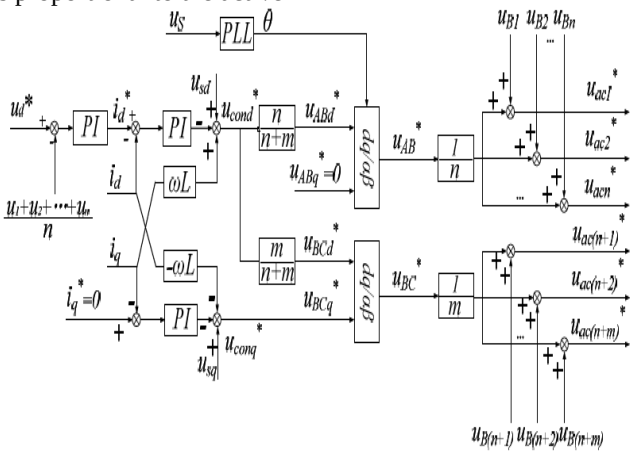

Fig.13. Control strategy based on the single-phase dq transformation.

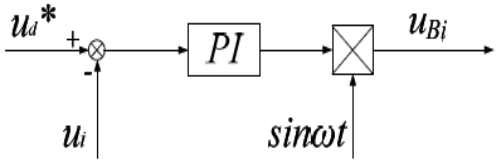

Fig.14. Diagram of output dc voltage balancing.

component of its ac voltage. Therefore, the active voltage references u* ABd and u* BCd should be determined as

$$\begin{cases} u^*_{ABq} = 0 \\ u^*_{BCq} = u^*_{\mathrm{conq}} \end{cases} \quad (28)$$

$$\begin{cases} u^*_{\mathrm{ABd}} = \dfrac{n}{n+m} u^*_{cond} \\ u^*_{BCd} = \dfrac{m}{n+m} u^*_{cond}. \end{cases} \quad (29)$$

By employing two single-phase inverse dq transformations, the ac voltage references, u* AB and u* BC, are both obtained. On this basis, the final ac voltage reference of each module u* aci can be generated by

$$\begin{cases} u^*_{\mathrm{aci}} = \dfrac{u^*_{\mathrm{AB}}}{n} + u_{\mathrm{Bi}}, \quad i = 1, 2, \ldots, n \\ u^*_{\mathrm{aci}} = \dfrac{u^*_{\mathrm{BC}}}{m} + u_{\mathrm{Bi}}, \quad i = (n+1), (n+2), \ldots, (n+m) \end{cases} \quad (30)$$

where uBi is the dc voltage balancing signal.

Fig14 describes the dc voltage balancing control diagram [3], [4]. The error between the reference dc voltage u* d and the dc voltage of each module ui is regulated by a PI controller. The output of the PI controller is then multiplied by "sin ωt" to produce the balancing signal uBi. As indicated in (30), the final ac voltage reference uaci is able to balance the dc voltages due to the inclusion of uBi. Through the proposed control strategy, the phasor relationship shown in Fig11 can be guaranteed, thus enabling the revised single-phase CBR to realize unity power factor rectification without suffering the input current zero-crossing distortion.

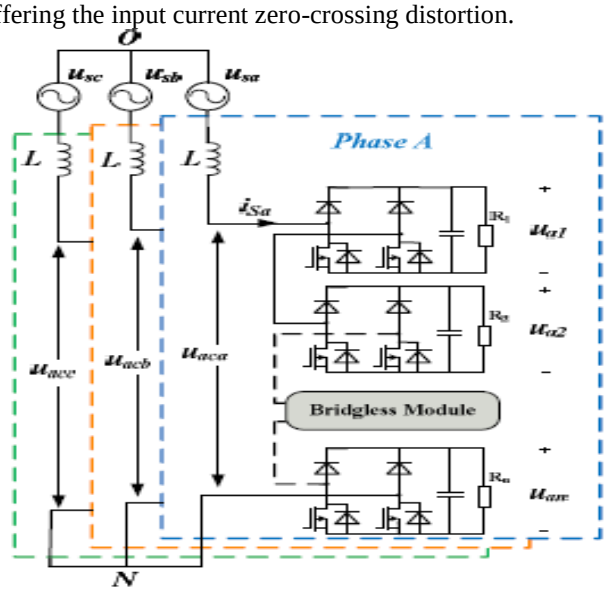

Fig.15. Topology of the three-phase CBR.

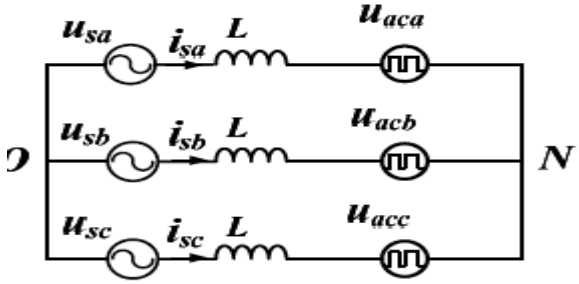

Fig.16. Equivalent ac side circuit of the three-phase CBR.

V. DISCUSSION ON INPUT CURRENT ZERO-CROSSING DISTORTION OF THE THREE-PHASE CBR

As shown in Fig. 15, the proposed single-phase CBR can be expanded to a three-phase structure. The equivalent ac side circuit is depicted in Fig. 16 and the mathematical model can be expressed as

$$\begin{cases} L\dfrac{di_{sa}}{dt} = u_{sa} - u_{aca} - u_{NO} \\ L\dfrac{di_{sb}}{dt} = u_{sb} - u_{acb} - u_{NO} \\ L\dfrac{di_{sc}}{dt} = u_{sc} - u_{acc} - u_{NO} \end{cases} \quad (31)$$

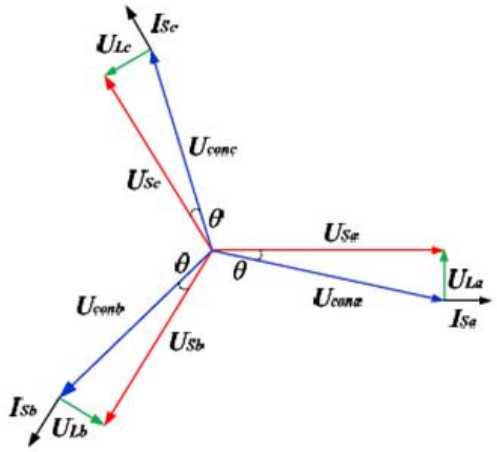

Fig. 17. AC side phasor diagram of the three-phase CBR under the unity power factor operation.

where uack is the sum of ac voltages of the bridgeless modules in Phase k, k = a, b, c; uNO is the neutral point voltage. Define uconk as the total ac voltage of Phase k with respect to the power source neutral point (Node O). Then the relationship between uNO, uack, and uconk is given as

$$u_{conk} = u_{ack} + u_{NO} \quad (31)$$

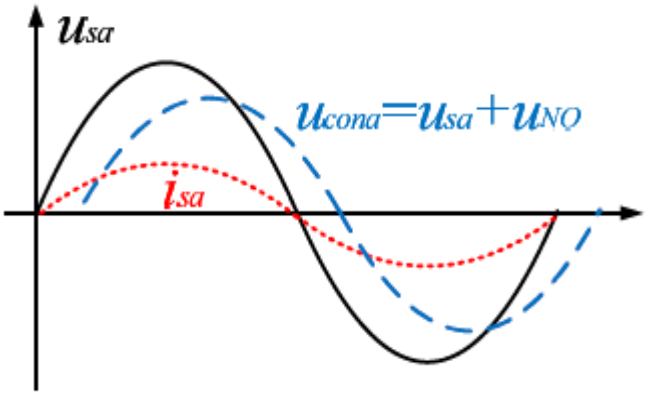

Fig. 18. Phase a ac side waveforms of the three-phase CBR under the unity power factor.

By regulating uconk at their references uconk*, the power factor and the input currents can be controlled. Due to the unidirectional conduction property of the diodes, isk and uack are always in phase. However, as depicted in Fig. 17, Uconk lags Isk by θ when the CBR is operating under the unity power factor. As a result, during a short period after the current zero-crossing, isk and uconk need to have opposite polarities. Equation (32) indicates that uconk is the sum of uack and uNO.Therefore, even though uack has to be in the same direction as isk, uNO can be in the opposite direction so that uconk can still follow its reference. In this way, the current zero-crossing distortion can be mitigated. Assuming that isa is turning from positive to negative. At this instant, the ac voltage reference u* cona is positive. Due to the unidirectional conduction property, uaca can only be zero. However, a positive uNO can be generated to synthesize the desired u* cona. For the other two phases, uconb anduconc can still follow their references. Consequently, as shown in Fig. 18, the unity power factor can be achieved with attenuated input current zero-crossing distortion.

VI. SIMULATION RESULTS

To verify the proposed theories, simulations are carried out in the MATLAB/Simulink environment. A single-phase CBR model composed of two modules is built according to Table I. Fig. 19 shows the input voltage and input current of the single-phase CBR under the traditional control, which requires the unity power factor to be achieved. The input current is in phase with the input voltage. However, severe current distortion appears at the zero-crossings. To eliminate the undesirable distortion, the improved control strategy is then employed. As can be seen from Fig. 20, by making the input current lag the input voltage by ϕ, the input current distortion are avoided. Fig. 21 further indicates that under the improved control, dc voltages of the two cascaded modules are well balanced, which guarantees the safe and stable operation of the rectifier system. If a unity power factor is strictly required, the improved control strategy cannot be used. Under this circumstance, the revised single-phase CBR topology is an alternative.

TABLE I: Simulation Parameters For The Single-Phase CBR

Parameter	Quantity	Values
u_S	input voltage	220V
u_1	output DC voltage of Module 1	300V
u_2	output DC voltage of Module 2	300V
f_s	switching frequency	10 kHz
L	boost inductance	1.5mH
R_1	load resistance of Module 1	20Ω
R_2	load resistance of Module 2	20Ω
C_1	DC capacitance of Module 1	2200μF
C_2	DC capacitance of Module 2	2200μF

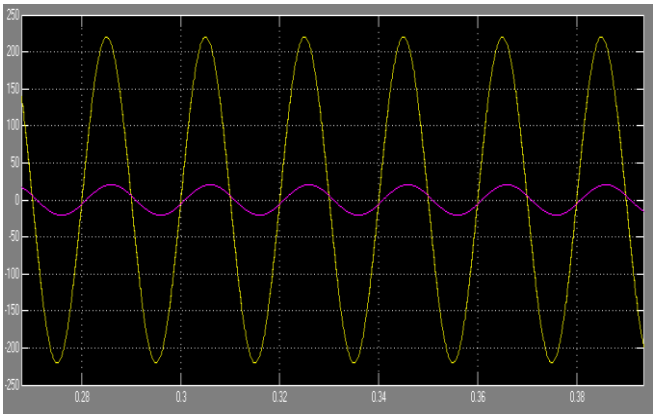

Fig.19. Input current and input voltage of the single-phase CBR under the traditional control.

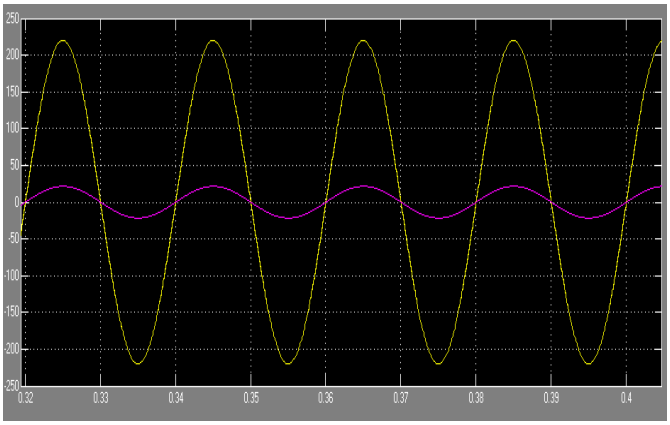

Fig.20. Input current and input voltage of the single-phase CBR under the improved control.

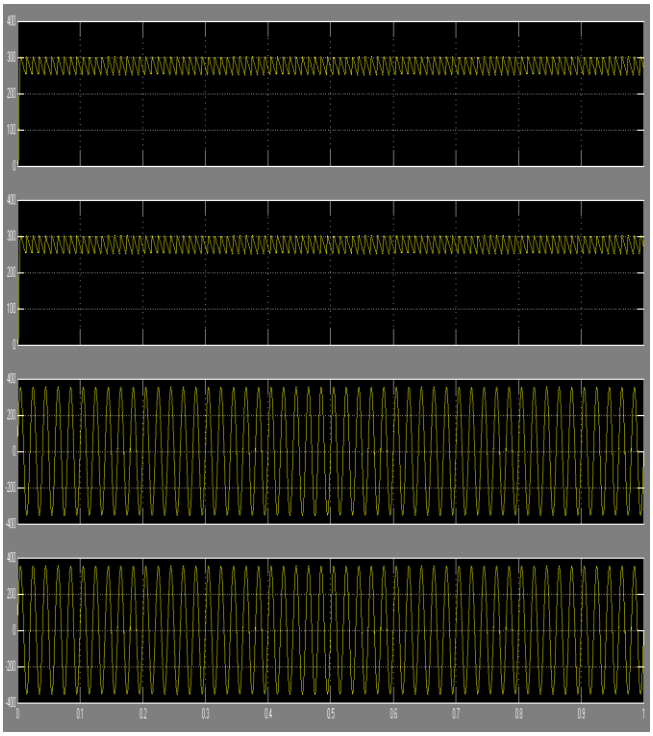

Fig.21. Output dc voltages and the ac voltages of the single-phase CBR under the improved control.

VII. CONCLUSION

A CBR is presented to reduce the number of fully controlled switches and simplify the system complexity. The basic principles of the proposed topology are analyzed. To achieve a satisfactory power factor and eliminate the input current zero-crossing distortion, an improved control strategy and a revised topology are presented. For the CBR under the improved control, the method of selecting the maximum boost inductance considering an acceptable power factor is derived. For the revised single-phase CBR, the determination method of the topology configuration is also given. In addition, this paper explains the ability of the three-phase CBR to attenuate the current distortion while realizing unity power factor rectification. Finally, the simulation results validated the proposed theories.

VIII. REFERENCES

[1] Z. Li, P. Wang, H. Zhu, Z. Chu, and Y. Li, "An improved pulse width modulation method for chopper-cell-based modular multilevel converters," IEEE Trans. Power Electron., vol. 27, no. 8, pp. 3472–3481, Aug. 2012.

[2] S. M. Park and S.-Y. Park, "Versatile control of unidirectional AC–DC boost converters for power quality mitigation," IEEE Trans. Power Electron., vol. 30, no. 9, pp. 4738–4749, Sep. 2015.

[3] H. Iman-Eini, S. Farhangi, M. Khakbazan-Fard, and J.-L. Schanen, "Analysis and control of a modular MV-to-LV rectifier based on a cascaded multilevel converter," J. Power Electron., vol. 9, no. 2, pp. 133–145, Mar. 2009.

[4] R. Nagarajan and M. Saravanan, "Performance analysis of a novel reduced switch cascaded multilevel inverter," J. Power Electron., vol. 14, no. 1, pp. 48–60, Jan. 2014.

[5] J. Venkat, A. Shukla, and S. V. Kulkarni, "Operation of a three phase solid state-Transformer under unbalanced load conditions," in Proc. IEEE Int. Conf. Power Electron., Drives Energy Syst. (PEDES), Dec. 2014, pp. 1–6.

[6] J. Shi, W. Gou, H. Yuan, T. Zhao, and A. Q. Huang, "Research on voltage and power balance control for cascaded modular solidstate transformer," IEEE Trans. Power Electron., vol. 26, no. 4, pp. 1154–1166, Apr. 2011.

[7] Z. Ji, J. Zhao, Y. Sun, X. Yao, and Z. Zhu, "DC voltage balancing control for cascaded grid-connected inverters by injecting zero-sequence and negative-sequence voltages," in Proc. CSEE, Sep. 2013, vol. 33. no. 21, pp. 9–17.

[8] G. Zhang, "Research on cascaded H-bridge rectifier stage and balance control for DC-link capacitor voltages," Ph.D. dissertation, School Mech. Electron. Inf. Eng., China Univ. Mining Technol., Beijing, China, 2012.

[9] H. Akagi and S. Inoue, "Medium-voltage power conversion systems in the next generation," in Proc. IEEE Power Electron. Motion Control Conf. (IPEMC), Aug. 2006, pp. 1–8.

[10] J. Wang, "Research on cooperative control of cascaded H-bridge multilevel converter," Ph.D. dissertation, School Mech. Electron. Inf. Eng., China Univ. Mining Technol., Beijing, China, 2015.

.